

<https://doi.org/10.1038/s41541-025-01337-0>

# mRNA-LNP vaccine encoding CDV hemagglutinin confers effective protection in raccoon dogs

Check for updates

Chengqi Zhang<sup>1,2,4</sup>, Tiyun Han<sup>3,4</sup>, Dingrui Guo<sup>1,2</sup>, Shuangshuang Li<sup>2</sup>, Wenyu Cao<sup>1,2</sup>, Xiaolan Guo<sup>1,2</sup>, Zichaung Zhang<sup>1</sup>, Jiajia Liu<sup>1,2</sup>, Yajie Sun<sup>1,2</sup>, Liwen Xu<sup>1,2</sup>, Ping Ma<sup>1,2</sup>, Mengwei Xu<sup>3</sup>, Jing Li<sup>3</sup>, Shi Xu<sup>3</sup>✉, Bo Hu<sup>1,2</sup>✉ & Xue Bai<sup>1,2</sup>✉

Canine distemper virus (CDV) is a highly contagious morbillivirus that causes severe disease in carnivores, with raccoon dogs (*Nyctereutes procyonoides*) serving as major reservoirs for transmission. To address the limitations of current vaccines—such as virulence reversion, multiple doses, and poor efficacy in raccoon dogs—we developed a novel mRNA–lipid nanoparticle (LNP) vaccine encoding a secreted, tetrameric CDV hemagglutinin (H) protein fused to a signal peptide and Tetrabrachion domain to enhance stability and immunogenicity. The vaccine showed high purity, uniform particle size (~108 nm), and efficient *in vivo* expression of glycosylated H protein. In BALB/c mice, it induced strong H-specific IgG and increased splenic CD4<sup>+</sup> T cells, suggesting a Th-skewed immune response. In raccoon dogs, high neutralizing antibody titers were maintained post-immunization, and all vaccinated animals survived lethal CDV challenge, whereas controls showed 100% mortality. Compared with a live-attenuated CDV vaccine, the mRNA–LNP vaccine markedly reduced clinical signs, preserved intestinal integrity, and nearly eliminated viral RNA in mucosal and systemic tissues. This study provides the first evidence that an mRNA-LNP vaccine encoding CDV hemagglutinin can confer complete protection against CDV challenge in raccoon dogs, highlighting its potential for veterinary and wildlife disease prevention.

Canine distemper virus (CDV) is a highly contagious morbillivirus that infects a broad spectrum of carnivores and causes systemic disease characterized by respiratory, gastrointestinal, and neurological manifestations<sup>1–3</sup>. Although live-attenuated and inactivated vaccines have successfully reduced CDV incidence in domestic dogs, spillover into wildlife and fur-farmed species—particularly raccoon dogs—continues to cause recurrent outbreaks associated with high morbidity and mortality<sup>4–6</sup>. Raccoon dogs (*Nyctereutes procyonoides*), which are widely farmed for fur in East Asia and Europe, are especially vulnerable, exhibiting nearly 100% mortality upon CDV infection under experimental conditions and serve as important reservoirs for virus transmission to other carnivores, including endangered species<sup>7–9</sup>.

CDV comprises a single serotype but nine recognized genotypes, including America-1, America-2, Europe-1/South America-1, Europe-2/Europe wildlife, Asia-1, Asia-2, Arctic, South America-2, and Southern Africa<sup>10–13</sup>. Among these, America-1 and America-2 correspond to vaccine

lineages, while the others represent wild-type field strains that cluster into two major phylogenetic branches. The amino acid homology of the H protein among different genotypes ranges from 89% to 100%. In China, three major genotypes—Asia-1, Asia-3, and Arctic—have been detected in dogs, foxes, raccoon dogs, and minks, with Asia-1 being the predominant epidemic lineage<sup>14,15</sup>.

Current CDV vaccines encompass live-attenuated strains (e.g., Nobivac® Canine 1-DAPPv), inactivated vaccines, and recombinant formulations. Live-attenuated vaccines (LAV) mimic natural infection and induce robust, long-lasting immunity without the need for repeated boosters; however, they carry risks of reversion to virulence and can cause disease in immunocompromised or highly susceptible hosts<sup>16</sup>. Inactivated vaccines, by contrast, eliminate the risk of back-mutation and are suitable for animals with weakened immune systems, but they generally require adjuvants and multiple immunizations to achieve sufficient protection. Recombinant

<sup>1</sup>Key Laboratory of Special Animal Epidemic Disease of the Ministry of Agriculture, Institute of Special Animal and Plant Sciences, Chinese Academy of Agricultural Sciences, Changchun, China. <sup>2</sup>Jilin Provincial International Cooperation Key Laboratory for Science and Technology Innovation of Special Animal and Plants, Institute of Special Animal and Plant Sciences, Chinese Academy of Agricultural Sciences, Changchun, China. <sup>3</sup>Nanjing Chengshi (TheraRNA) Biomedical Technology Co. Ltd., Nanjing, China. <sup>4</sup>These authors contributed equally: Chengqi Zhang, Tiyun Han.

✉ e-mail: [xushi@therarna.cn](mailto:xushi@therarna.cn); [hubo@caas.cn](mailto:hubo@caas.cn); [baixue01@caas.cn](mailto:baixue01@caas.cn)

canarypox-vectored vaccines expressing the H and F glycoproteins—key mediators of viral entry, immune evasion, and vaccine-induced protection—have also been explored<sup>17,18</sup>. Similarly, subunit or recombinant protein vaccines targeting specific CDV antigens avoid the risk of reversion but still depend on adjuvants or multiple doses to induce durable immunity<sup>19</sup>. DNA vaccines encoding H and F proteins, either alone or in combination with cytokines, have shown the ability to elicit both T- and B-cell responses<sup>20</sup>, yet efficient delivery of DNA vectors into host cells remains a major technical hurdle. More recently, subunit vaccines based on bacterium-like particle (BLP) platforms displaying CDV antigens have demonstrated the capacity to induce robust humoral and cellular immune responses in mice and dogs<sup>21,22</sup>. While recombinant vectored vaccines offer improved safety profiles, they may show variable efficacy across species and pose challenges for large-scale production and cold-chain distribution<sup>23</sup>. Importantly, few vaccine platforms have been systematically evaluated in raccoon dogs, highlighting a critical gap in developing vaccines specifically tailored to this high-risk species<sup>24</sup>.

In research of CDV vaccines, the importance of animal models, especially those involving natural reservoirs such as raccoon dogs, is crucial for understanding CDV transmission dynamics. These models help elucidate virus shedding patterns, inter-species transmission, and the virus's role in cross-species outbreaks<sup>7</sup>. They are also essential for evaluating the efficacy of vaccine candidates, as they allow for testing in species that naturally harbor and spread the virus<sup>25</sup>. Furthermore, animal models enable the study of CDV's evolutionary potential, including antigenic variation and immune escape, which are critical for developing long-lasting vaccines<sup>5</sup>. By simulating real-world transmission scenarios and immune responses, these models offer vital insights for controlling CDV in both wildlife conservation and veterinary practice.

Messenger RNA (mRNA) vaccine technology has transformed human vaccinology by enabling rapid antigen design, strong immunogenicity, and a favorable safety profile<sup>26,27</sup>. Over the past five years, mRNA constructs encoding viral glycoproteins—such as those of rabies, influenza, Zika—have induced high titers of neutralizing antibodies, robust CD4<sup>+</sup>/CD8<sup>+</sup> T-cell responses, and complete protection in murine and nonhuman primate challenge models<sup>28–30</sup>. Although veterinary applications of mRNA vaccines remain at an early stage, encouraging results in swine and poultry (e.g., mRNA influenza vaccines in pigs) suggest broad potential across animal species<sup>29,31</sup>. However, to date, no CDV mRNA vaccine has been evaluated in raccoon dogs, leaving a critical gap in translating mRNA platforms to high-impact veterinary pathogens.

In this study, we designed an mRNA encoding a secreted, tetrameric form of the CDV hemagglutinin (H) protein, fused to a signal peptide (SP) and the Tetrabrachion tetramerization domain (T $\beta$ tetra), to optimize antigen secretion, conformational stability, and immunogenicity. As one of the two surface glycoproteins of CDV (along with the fusion [F] protein), H protein mediates viral attachment to host receptors such as SLAM and nectin-4 and represents the most genetically variable CDV structural protein<sup>10,32</sup>. It harbors multiple neutralizing antibody epitopes, particularly within the receptor-binding domain, making it the principal target of virus-neutralizing immune responses and a key determinant of host range and immune evasion<sup>33</sup>. By contrast, the F protein primarily mediates membrane fusion between the virus and the host cell<sup>34</sup>. Although the F protein can contribute to vaccine design in combination with H, it exists in both pre-fusion and postfusion conformations, with neutralizing epitopes restricted to the pre-fusion state<sup>35</sup>. Given these structural constraints, the H protein was selected as the primary vaccine antigen, as it plays a pivotal role in CDV infection and immune recognition. Compared with internal proteins such as the nucleocapsid (N) or phosphoprotein (P), which are mainly involved in viral replication, H elicits stronger humoral immunity and is therefore better suited for prophylactic vaccine design<sup>8,36,37</sup>.

The mRNA construct was synthesized in vitro and encapsulated in lipid nanoparticle (LNP) composed of ionizable lipid, 1,2-distearoyl-sn-glycero-3-phosphocholine (DSPC), cholesterol, and 1,2-dimyristoyl-rac-glycerol-3-methoxypolyethylene glycol 2000 (DMG-PEG 2000). The

resulting formulation was characterized for particle size and in vivo delivery efficiency<sup>38,39</sup>. We then assessed the immunogenicity, safety, and protective efficacy of the CDV-H mRNA-LNP vaccine in both BALB/c mice and raccoon dogs<sup>30</sup>. Specifically, we aimed to determine whether this platform could (i) elicit high titers of CDV-neutralizing antibodies, (ii) induce appropriate T-cell responses, (iii) confer protection against lethal CDV challenge, and (iv) mitigate systemic and tissue-level pathology in a naturally susceptible host species. By addressing these goals, this study provides the first demonstration of an mRNA vaccine against CDV in raccoon dogs, advancing both the field of veterinary mRNA vaccinology and offering a promising strategy for controlling CDV in wildlife reservoirs.

## Results

### In vivo delivery and in vitro expression of CDV-H mRNA-LNP

The mRNA encoding a secreted, tetrameric form of the CDV H protein was successfully synthesized and encapsulated in LNP. As shown in Fig. 1A, the construct consists of an N-terminal SP, the T $\beta$ tetra, and the ECD of H. Microfluidic electrophoresis of the in vitro-transcribed mRNA revealed a single predominant full-length peak with 90.2% purity (Fig. 1B), indicating minimal degradation or truncation. DLS analysis demonstrated that mRNA-LNP had a mean hydrodynamic diameter of 108.52 nm with a PDI of 0.063 (Fig. 1D), reflecting a uniform nanoparticle population. The autocorrelation function ( $g_2-1$ ) curve decayed smoothly with an intercept of 0.96 (Fig. 1E), confirming high-quality measurements and strong signal-to-noise ratio. In vivo delivery was evaluated by intramuscular injection of fluorescently labeled mRNA-LNP into mice. Bioluminescence imaging at 6 h post-injection showed fluorescence restricted to the injection site (Fig. 1C), demonstrating efficient local retention without detectable off-target distribution.

In vitro expression was verified in CHO cells transfected with mRNA-LNP. At 24 h post-transfection, indirect immunofluorescence with a rabbit anti-CDV polyclonal primary antibody and FITC-conjugated goat anti-rabbit IgG antibody revealed strong green fluorescence in transfected cells, with DAPI counterstaining confirming intact nuclear morphology (Fig. 1F). WB analysis of cell lysates harvested at 24 hours post-transfection detected a distinct band at ~95 kDa (Fig. 1G, full-length blot shown in Fig. S1). Although the unmodified H protein is predicted to be 73.1 kDa, the higher apparent molecular weight corresponds to its glycosylated form, consistent with the presence of N-linked glycosylation sites within the H sequence.

Together, these findings demonstrate that the CDV-H mRNA-LNP vaccine exhibits high purity, forms uniform nanoparticles, achieves efficient in vivo delivery with localized retention, and directs robust expression of glycosylated H protein in vitro.

### CDV-H mRNA-LNP induces antigen-specific humoral and cellular immune responses in mice

To evaluate the immunogenicity of the CDV-H mRNA-LNP vaccine, BALB/c mice were immunized on Days 0 and 21, with serum samples collected at 21, 28, and 42 dpi. As shown in Fig. 2B, the level of CDV H protein-specific antibodies in the mRNA-H vaccinated group was significantly elevated compared to the PBS control on Day 21 and remained at high levels through Day 42, as determined by indirect ELISA. Indirect immunofluorescence analysis further confirmed these findings (Fig. 2C). Sera from both the mRNA-H group and LAV group specifically recognized CDV-infected Vero cells, as indicated by green fluorescence, demonstrating the successful induction of CDV-specific antibodies.

To assess vaccine-induced cellular immunity, splenic lymphocytes were analyzed by flow cytometry at 42 dpv. As shown in Fig. 2D, the proportion of CD4<sup>+</sup> T cells was significantly increased in the mRNA-H group compared with the PBS control, whereas no significant difference was observed in CD8<sup>+</sup> T cells. These results indicate that mRNA-H vaccine predominantly activates CD4<sup>+</sup> T helper cells, consistent with a humoral immunity-biased response.

Collectively, these results demonstrate that the CDV-H mRNA-LNP vaccine elicits robust antigen-specific antibody responses and induces a helper T cell-dominant immune profile in mice.

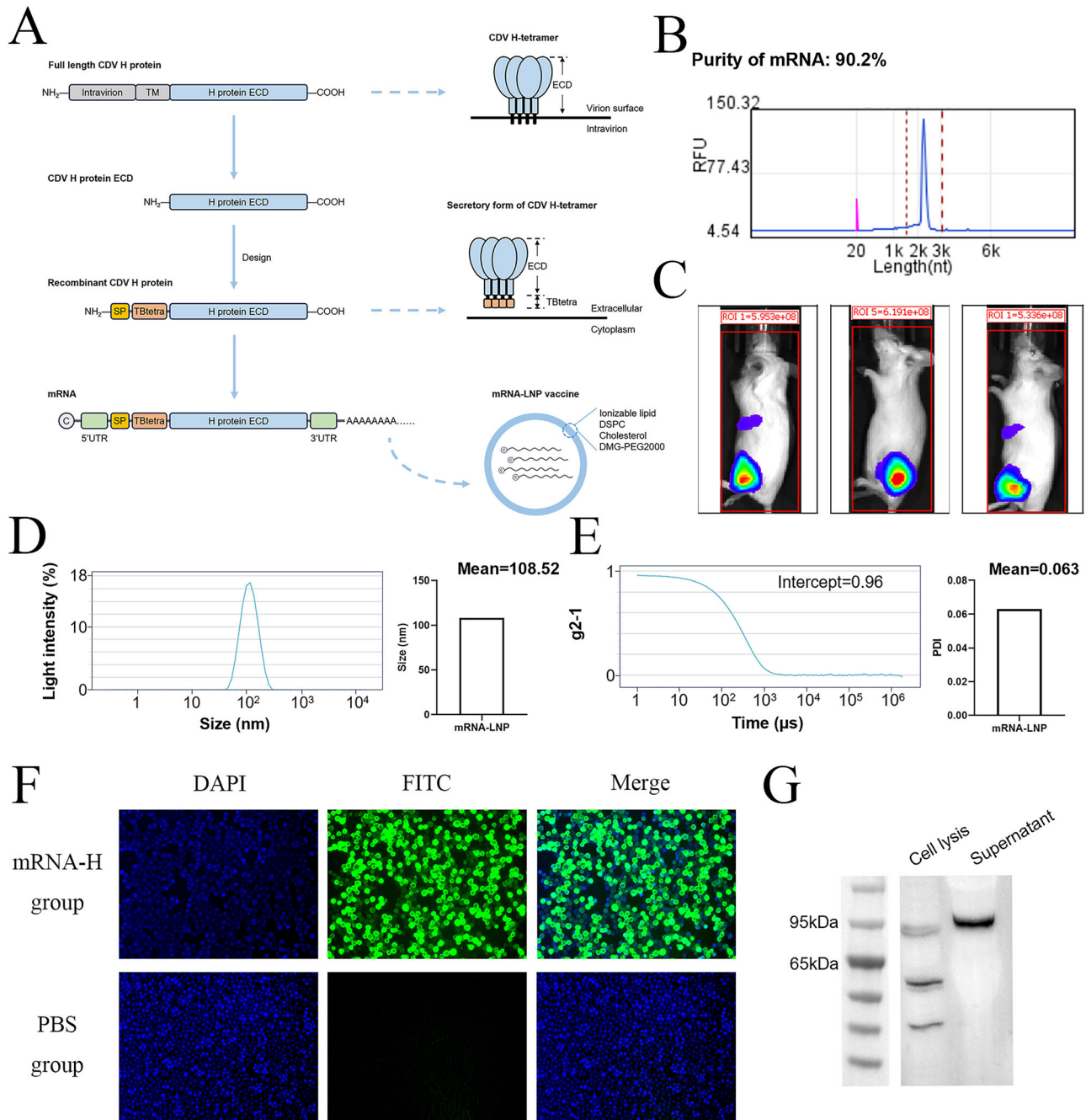


**Fig. 1 | In vivo fluorescent localization and delivery distribution of CDV-H mRNA-LNP vaccine.** **A** Schematic representation of the mRNA construct encoding the secreted, tetrameric form of the canine distemper virus (CDV) hemagglutinin (H) protein. The construct contains a signal peptide (SP), tetrabrachion tetramerization domain (Tβtetra), and extracellular domain (ECD) of the H protein. The mRNA was synthesized in vitro and encapsulated in lipid nanoparticle (LNP) consisting of ionizable lipid, DSPC, cholesterol, and DMG-PEG2000. **B** Purity analysis of in vitro transcribed mRNA by microfluidic electrophoresis. **C** In vivo bioluminescence imaging of mice following intramuscular injection of labeled mRNA-LNP. **D** Size distribution and polydispersity index (PDI) of mRNA-LNP

determined by dynamic light scattering (DLS). **E** DLS correlation function ( $g^2-1$ ) curve and intercept analysis. Time ( $\mu$ s) on the x-axis reflects the delay time over which particle motion remains correlated. **F** In vitro validation of H protein expression by indirect immunofluorescence. CHO cells transfected with mRNA-LNP were stained with rabbit polyclonal anti-CDV primary antibody and FITC-conjugated goat anti-rabbit IgG secondary antibody (green), with nuclear counterstained by DAPI (blue). **G** Western Blot (WB) analysis of H protein expression in cell lysates. At 24 h post-transfection with mRNA-LNP, cellular proteins were extracted and analyzed by WB.

**Assessment of safety and immunogenicity of the mRNA-H vaccine in raccoon dogs**

To evaluate the safety profile of the CDV-H mRNA-LNP vaccine, raccoon dogs were monitored following intramuscular immunization. As shown in Fig. 3B, no signs of local inflammation or lesions were observed at the injection site during the observation period. Clinical evaluations, including behavior, appetite, and fecal output (Fig. 3C–E), revealed no abnormalities,

and body temperature remained within the physiological range (Fig. 3F). These findings indicate that the vaccine was well tolerated and did not cause detectable stress or adverse clinical manifestations.

Immunogenicity was subsequently assessed. On Day 21 post-immunization, both the mRNA-H and LAV groups exhibited significantly elevated CDV-specific antibody levels compared with the PBS control (Fig. 3G). Consistently, neutralizing antibody titers measured on Day 28 were

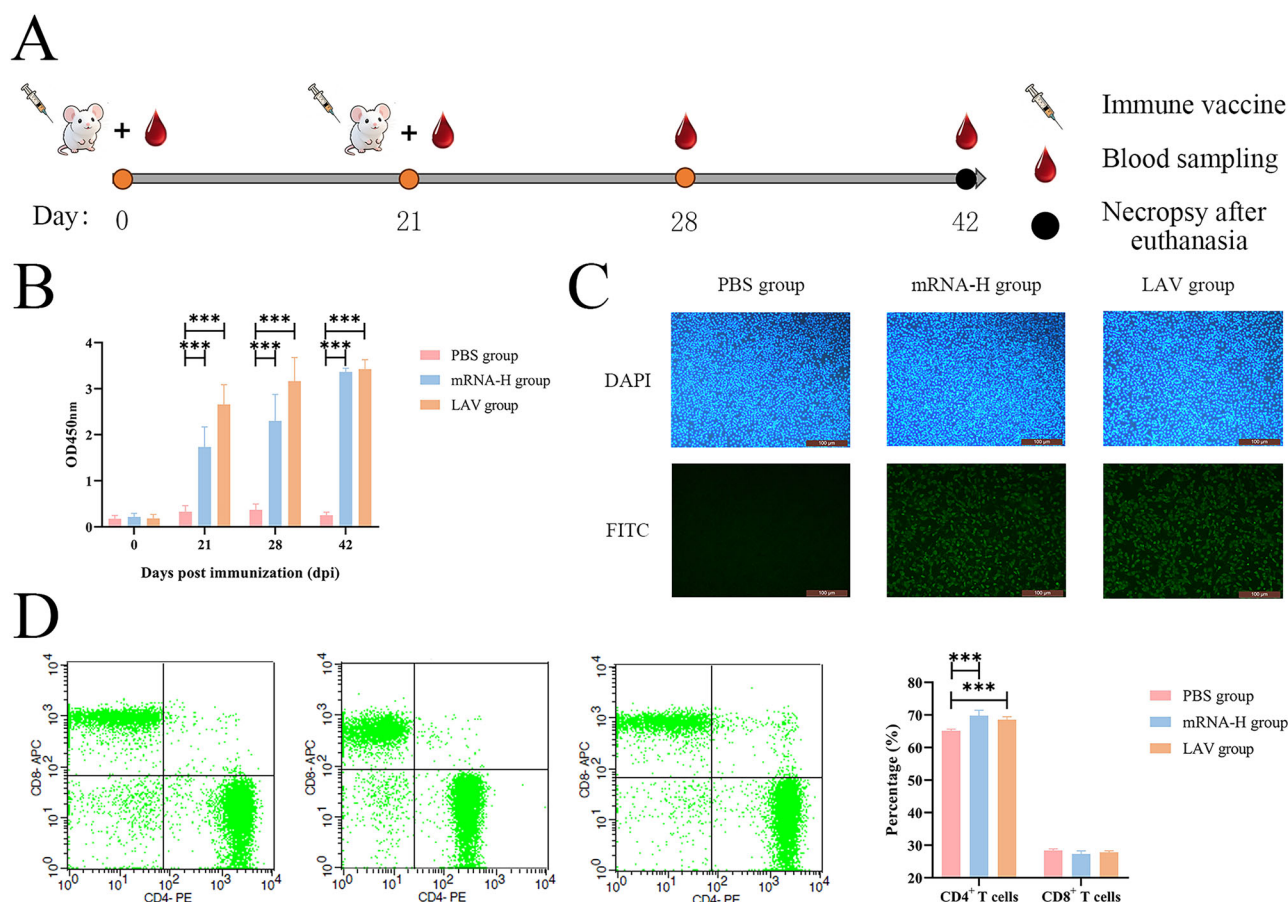


**Fig. 2 | Evaluation of immune responses induced by the CDV-H mRNA vaccine in mice.** **A** Schematic of immunization schedule. Mice received intramuscular injections of the formulated mRNA vaccine on Days 0 and 21. Blood samples were collected from the tail vein on Days 21, 28, and 42. All animals were euthanized for tissue collection at 42 days post-immunization (dpi). **B** Detection of CDV-specific antibodies in mouse sera. Levels of H protein-specific antibodies were measured by indirect ELISA. **C** Indirect immunofluorescence validation of vaccine-induced

antibodies. Serum antibodies from vaccinated mice specifically recognized CDV antigens in Vero cells, visualized using FITC-conjugated secondary antibody (green). Cell nuclei were counterstained with DAPI (blue). **D** Analysis of splenic lymphocyte subsets. Splenic lymphocytes collected at 42 dpi were analyzed by flow cytometry. A total of  $1 \times 10^5$  CD3<sup>+</sup> lymphocytes were gated to quantify CD4<sup>+</sup> and CD8<sup>+</sup> T cell subpopulations. Data are presented as mean  $\pm$  SEM ( $n = 5$  per group). Statistical significance is indicated as \* $P < 0.05$ , \*\* $P < 0.01$ , and \*\*\* $P < 0.001$ .

significantly higher in both vaccinated groups, confirming the induction of functional antiviral antibodies (Fig. 3H). Moreover, flow cytometry analysis demonstrated a significant increase in the proportion of CD4<sup>+</sup> T cells in the mRNA-H group relative to the PBS group, whereas CD8<sup>+</sup> T frequencies remained unchanged (Fig. 3I). These results suggest that the mRNA-H vaccine primarily induces a humoral immunity-oriented response.

**Protective efficacy of the CDV-H mRNA vaccine against virulent CDV challenge in raccoon dogs**

To assess the protective efficacy, raccoon dogs were challenged with virulent CDV following immunization. As shown in the survival curve (Fig. 4A), all animals in the mRNA-H and LAV groups survived, achieving 100% protection, whereas all animals in the PBS group succumbed by Day 11 dpc.

Body temperature monitoring (Fig. 4B) showed that vaccinated animals maintained stable temperatures, while the PBS controls exhibited a marked decline beginning at 9 dpc. Clinical observations (Fig. 4C) indicated normal activity and mental status in vaccinated groups, whereas the PBS group displayed lethargy. Food intake remained stable in the mRNA-H and LAV groups but declined in PBS controls (Fig. 4D). Fecal assessment (Fig. 4E) revealed that diarrhea developed in PBS animals from Day 6, with mild diarrhea observed in the LAV group at Day 7, while the mRNA-H group maintained normal fecal consistency. Similarly, mucosal symptoms (Fig. 4F) appeared in all groups by Day 6 but progressed more severely in the

LAV group by Day 8, whereas the mRNA-H group exhibited only mild signs.

Viral RNA quantification from rectal swabs (Fig. 4G) demonstrated high viral shedding in PBS controls at the time of death. At 14 dpc, both vaccinated groups tested negative for CDV antigen, indicating effective viral clearance. Collectively, these results show that the CDV-H mRNA vaccine provided complete protection and superior clinical outcomes compared with the live-attenuated vaccine.

**Histopathological evaluation of brain, lung, and spleen tissues**

To assess organ-level protection following CDV challenge, gross and microscopic pathology was examined in raccoon dogs from each group. As shown in Fig. 5A, PBS animals displayed obvious pathological alterations, including swollen intestinal segments and reduced spleen size. In contrast, no gross abnormalities were observed in the mRNA-H group, and only mild changes were noted in the LAV group.

Histological analysis revealed pronounced differences in tissue integrity (Fig. 5B). In the brain, PBS controls exhibited severe neuronal edema, loosely stained cytoplasm, shrunken neurons with irregular morphology, and vascular congestion. The mRNA-H group showed only minimal edema with largely preserved neuronal architecture, while the LAV group presented with intermediate lesions characterized by mild edema and numerous hyperchromatic, shrunken neurons. Quantitative scoring

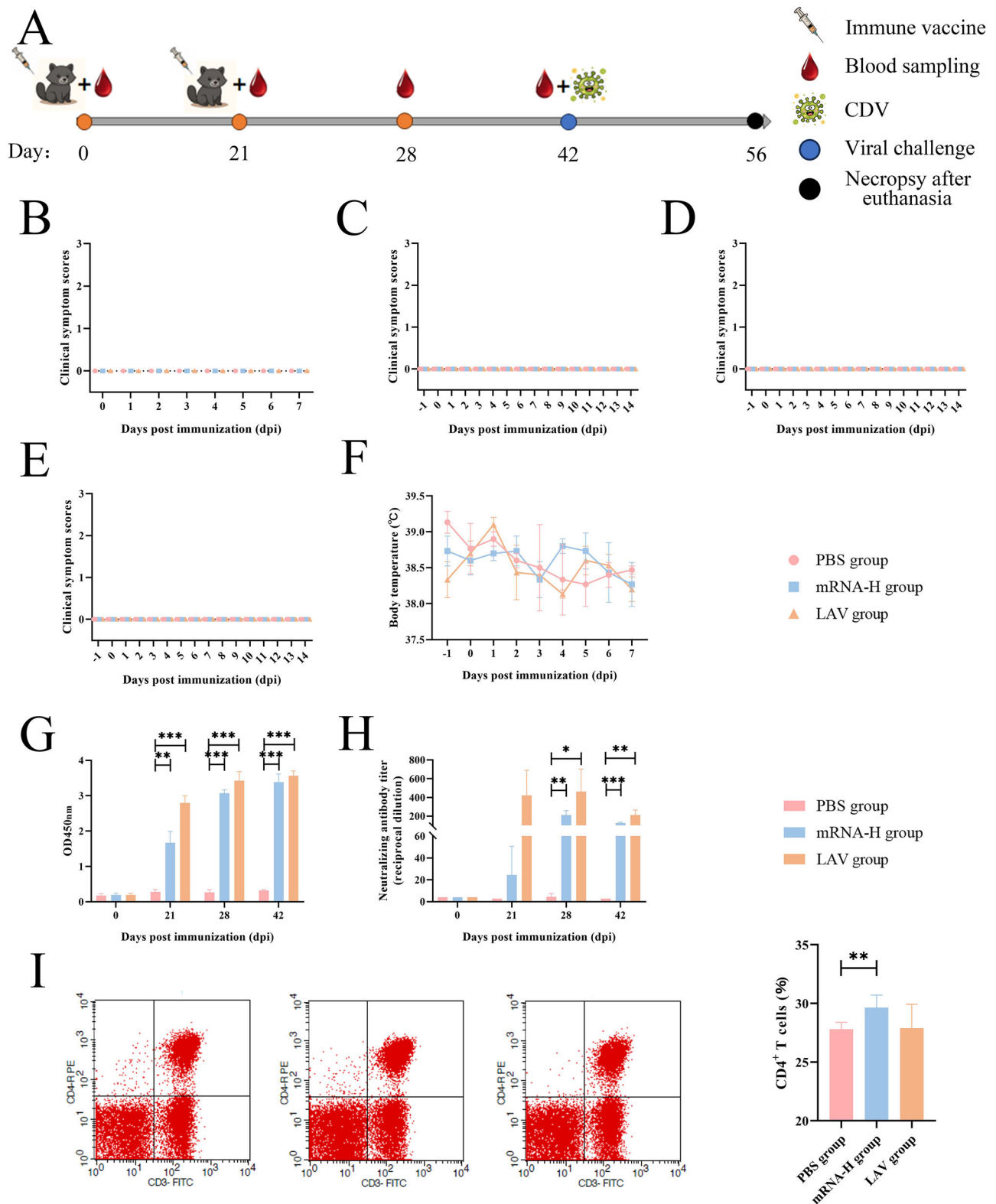


**Fig. 3 | Comprehensive evaluation of immunogenicity and safety of the CDV-H mRNA-LNP vaccine in raccoon dogs.** **A** Schematic of the immunization protocol. Animals received prime-boost vaccinations on Days 0 and 21, with sample collection at designated timepoints. **B–E** Clinical safety assessments. **B** Local reactogenicity at injection site scored as 0 = normal, 1 = mild erythema/edema, 2 = painful swelling, 3 = suppuration/ulceration. **C** Behavioral status: 0 = Normal activity, 1 = Lethargy/depression, 2 = Immobility. **D** Feed intake: 0 = Normal consumption, 1 = Hypophagia, 2 = Anorexia. **E** Fecal consistency: 0 = Normal, 1 = Soft stool, 2 = Watery

diarrhea, 3 = Hemorrhagic diarrhea. **F** Body temperature monitoring post-immunization. **G** Detection of CDV H-specific antibodies in serum by indirect ELISA. **H** Neutralizing antibody titers measured against a laboratory-preserved live CDV strain. **I** Flow cytometric analysis of peripheral blood lymphocytes subsets. A total of  $1 \times 10^5$  CD3<sup>+</sup> lymphocytes were gated to quantify CD4<sup>+</sup> T cell populations. Data are presented as mean  $\pm$  SEM ( $n = 5$  per group). Statistical significance is indicated as \* $P < 0.05$ , \*\* $P < 0.01$ , \*\*\* $P < 0.001$ .

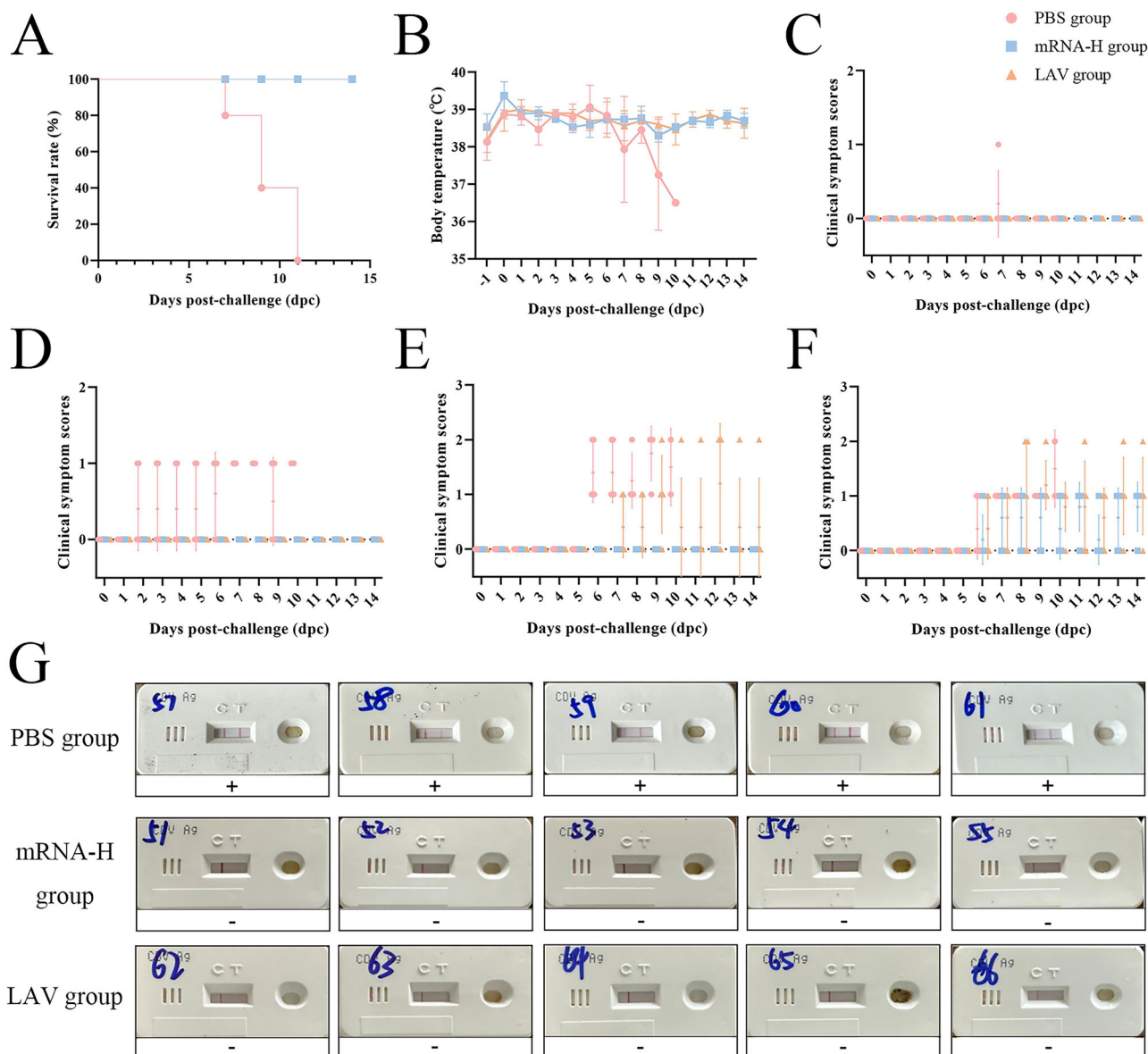


**Fig. 4 | Protective efficacy of the CDV-H mRNA vaccine in raccoon dogs after CDV challenge.** **A** Survival analysis following CDV challenge. Survival was monitored daily for 21 days post-challenge (dpc). **B** Body temperature dynamics after viral challenge. Axillary temperature was measured twice daily using infrared thermometry. **C–E** Clinical evaluation post-challenge, including behavioral status, feed intake, fecal consistency (scoring criteria as in Fig. 3B–E). **F** Ocular/nasal

discharge scoring. Grading scale: 0, normal; 1, mild hyperemia; 2, mucoid discharge; 3, purulent discharge. **G** Detection of CDV antigens in anal swabs. Rapid antigen test results are presented as negative (–) or positive (+), obtained either at 14 dpi for survivors or at the time of death for non-survivors. Data are presented as mean ± SEM ( $n = 5$  per group). Statistical significance is indicated as \* $P < 0.05$ , \*\* $P < 0.01$ , \*\*\* $P < 0.001$ .

confirmed significantly higher neuronal edema in PBS animals compared to the mRNA-H group ( $P < 0.01$ , Fig. 5C).

In the lungs, PBS animals exhibited moderate to severe alveolar wall thickening, epithelial disorganization, necrotic debris in bronchioles, and vascular congestion. The mRNA-H group demonstrated only mild wall thickening and inflammatory infiltration, with overall preservation of alveolar architecture. The LAV group showed lesions similar to PBS animals, with focal congestion and epithelial irregularities. Scoring indicated that alveolar wall thickening was significantly greater in PBS than LAV animals ( $P < 0.05$ ), while vascular congestion was more severe in PBS compared with both mRNA-H ( $P < 0.01$ ) and LAV ( $P < 0.001$ ) groups (Fig. 5D). In the spleen, PBS animals exhibited extensive necrosis and hemorrhage, whereas mRNA-H-vaccinated animals retained intact red and white pulp structures with minimal sinusoidal congestion. The LAV group also showed preserved splenic architecture with mild pathology. Quantitative analysis revealed significantly higher necrosis in

the PBS group compared to mRNA-H ( $P < 0.01$ ) and LAV ( $P < 0.001$ ) animals, and markedly greater vascular congestion in PBS animals than in both vaccinated groups (Fig. 5E).

Together, these findings demonstrate that the CDV-H mRNA-LNP vaccine conferred robust tissue-level protection against CDV-induced neuropathology, pulmonary inflammation, and splenic injury, with superior efficacy compared to the live-attenuated vaccine.

### Histopathological evaluation of CDV-induced lesions in major organs

Figure 6A shows the anatomical distribution of intestinal tissues and mesenteric lymph nodes, while Fig. 6B presents representative HE-stained sections. Pathological scores for each site are summarized in Fig. 6C–I. In the duodenum, the PBS-treated animals exhibited extensive epithelial cell shedding and necrosis, with significantly higher lesion scores compared to vaccinated groups ( $P < 0.01$ ). Both the mRNA-H and LAV groups displayed

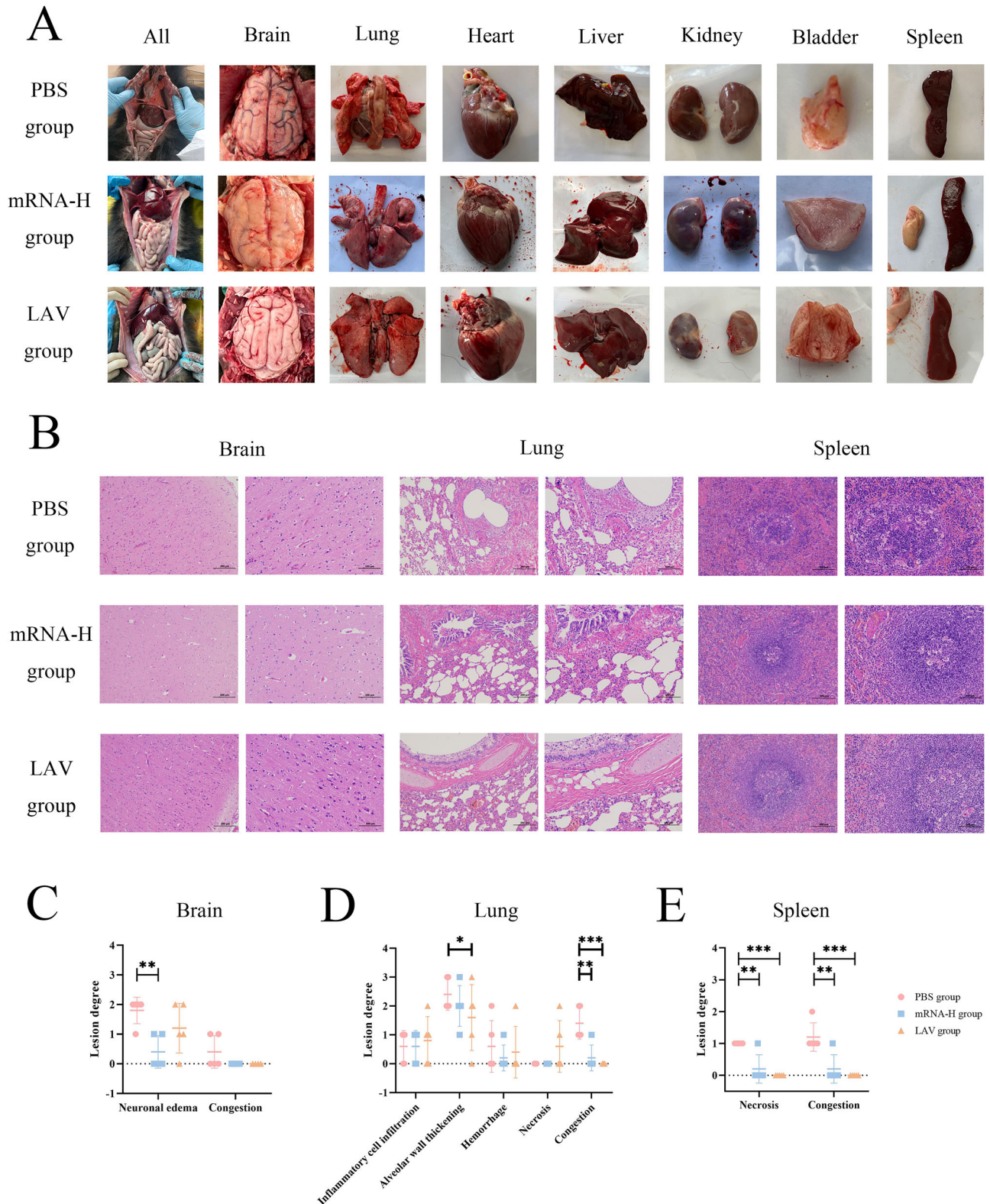


**Fig. 5 | Pathological assessment of CDV-infected raccoon dog tissues post-challenge.** **A** Gross pathology of major organs. Representative necropsy images illustrating morphological alterations. **B** Histopathological analysis (H&E Staining). Micrographs of brain, lung, and spleen sections showing characteristic lesions.

(C–E) Semi-quantitative pathological scoring. Grading scale: 0, normal; 1, minimal changes; 2, mild; 3, moderate; 4, severe. Data are presented as mean ± SEM ( $n = 5$  per group). Statistical significance is indicated as \* $P < 0.05$ , \*\* $P < 0.01$ , \*\*\* $P < 0.001$ .

markedly milder pathology, with the LAV group showing largely preserved architecture. In the jejunum and ileum, epithelial damage and inflammatory infiltration were again most severe in the PBS group. Notably, the mRNA-H group showed reduced epithelial loss and necrosis, particularly in the ileum

( $P < 0.05$ ), suggesting stronger protection. In the cecum and colon, the PBS animals demonstrated widespread mucosal erosion, glandular destruction, and necrotic debris accumulation. By contrast, the mRNA-H group largely maintained intact mucosal structures with limited necrosis, whereas the

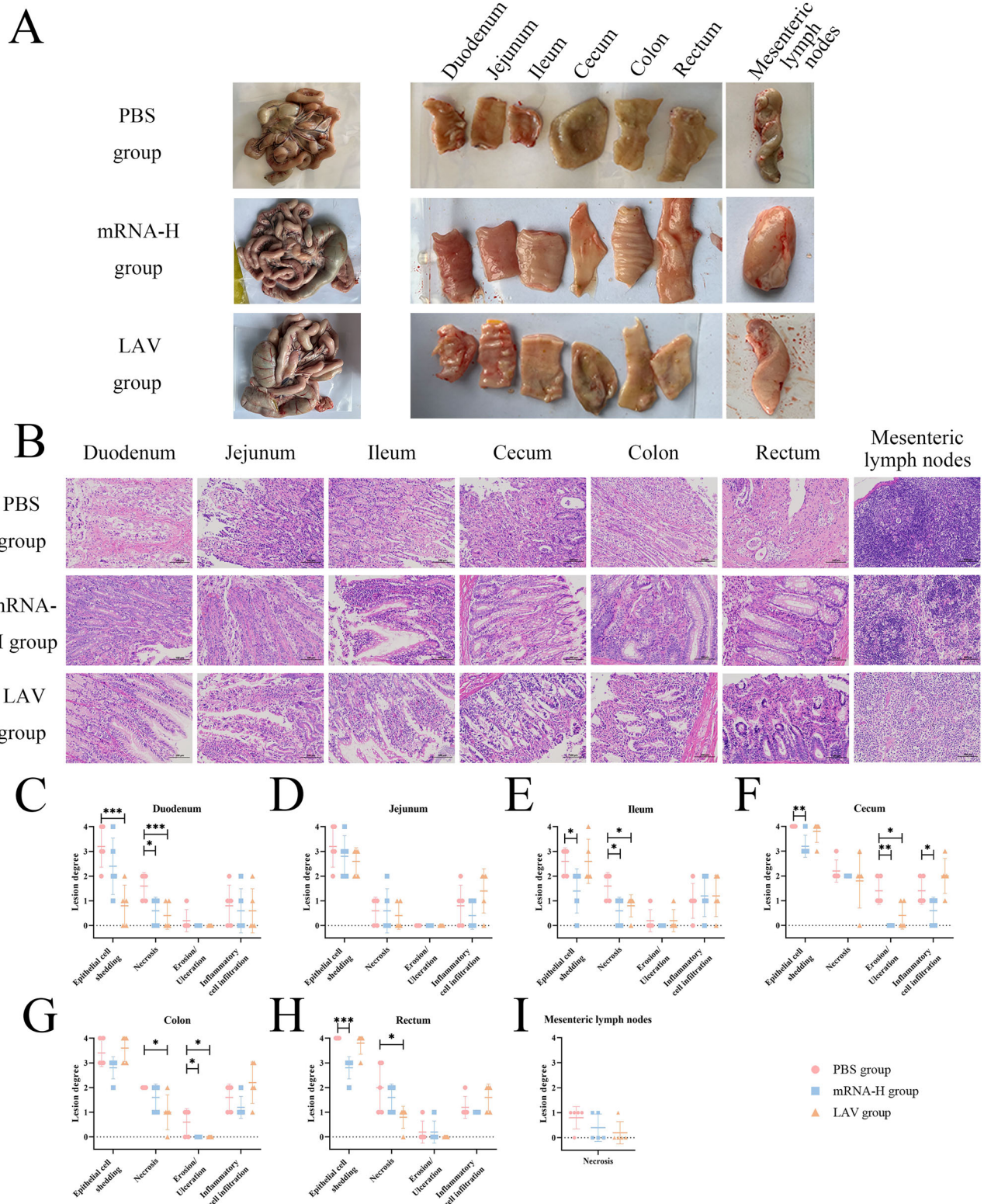


**Fig. 6 | Comprehensive pathological assessment of intestinal tract in CDV-infected raccoon dogs.** **A** Gross morphology of intestinal segments. Macroscopic examination of the duodenum, jejunum, ileum, cecum, colon, rectum, and mesenteric lymph nodes. **B** Histopathological analysis (H&E Staining). Representative micrographs showing pathological alterations across intestinal tissues.

**C–I** Semi-quantitative histopathological scoring of intestinal components. Grading scale: 0, normal; 1, minimal changes; 2, mild lesions; 3, moderate pathology; 4, severe damage. Data are presented as mean ± SEM (*n* = 5 per group). Statistical significance is indicated as \**P* < 0.05, \*\**P* < 0.01, \*\*\**P* < 0.001.

LAV group presented with moderate damage. In the rectum, the PBS animals exhibited severe epithelial loss, crypt destruction and focal ulceration (*P* < 0.05). Both vaccine groups showed attenuated lesions, with the mRNA-H group again demonstrating the most favorable outcomes. In the

mesenteric lymph nodes, the PBS animals exhibited smaller and fewer follicles with necrotic debris, indicative of impaired immune activity. Both vaccinated groups maintained relatively intact nodal architecture with only mild alterations.

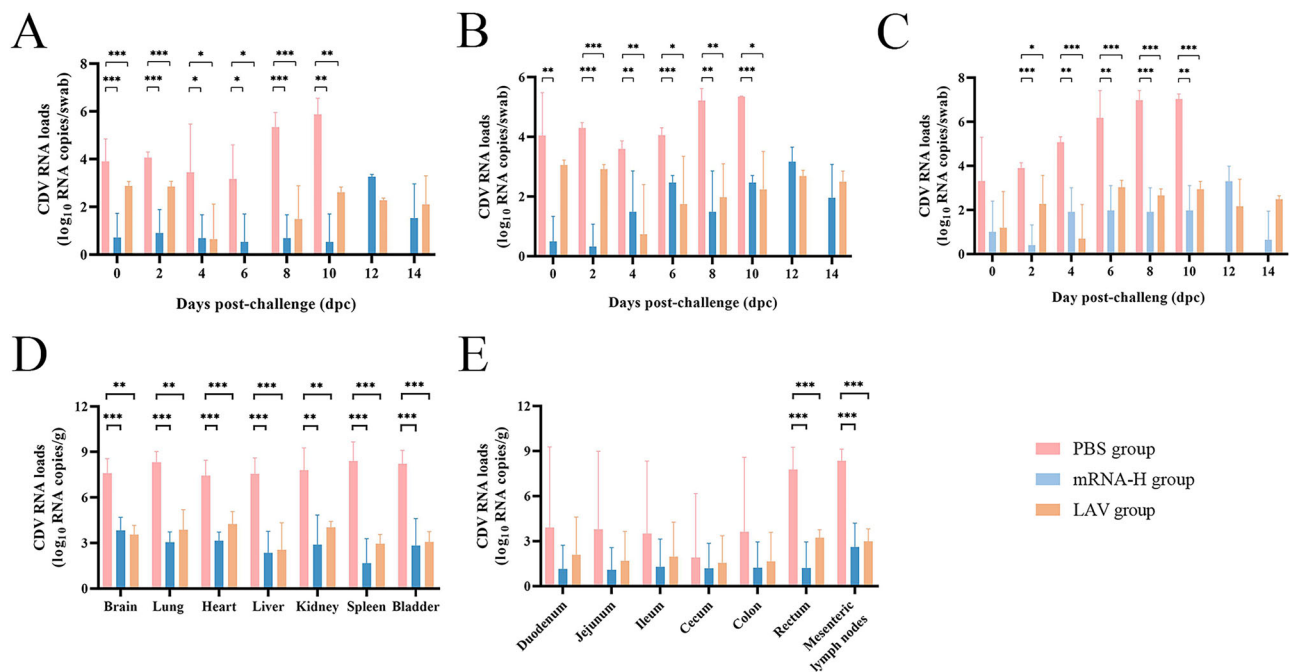


**Fig. 7 | CDV viral load distribution in swabs and tissues of raccoon dogs as measured by qPCR.** **A** CDV viral load in conjunctival swabs, expressed as log<sub>10</sub> RNA copies per swab. **B** CDV viral load in nasal swabs. **C** CDV viral load in anal swabs. **D** CDV viral RNA levels in major organs, including brain, lung, heart, liver, kidney, spleen, and bladder, collected at terminal endpoints. **E** CDV viral RNA levels in

intestinal tissues, including duodenum, jejunum, ileum, cecum, colon, and rectum. Data are presented as log<sub>10</sub> RNA copies per gram of tissue (or per swab where applicable). Data are presented as mean ± SEM (*n* = 5 per group). Statistical significance is indicated as \**P* < 0.05, \*\**P* < 0.01, \*\*\**P* < 0.001.

Overall, the PBS group displayed the most severe intestinal pathology across all segments. The mRNA-H vaccine significantly alleviated epithelial shedding, necrosis, and inflammation, showing enhanced protection compared with the live-attenuated vaccine.

**Viral load quantification by qPCR in swabs and tissues**

To assess viral replication and systemic dissemination following CDV challenge, viral RNA loads were measured in swab samples and tissues by quantitative RT-PCR. As shown in Fig. 7A–C, ocular, nasal, and anal swabs from PBS-treated animals displayed high RNA levels, peaking between 6 and 10 days dpc, consistent with extensive viral shedding. By Days 12 and 14, all PBS animals had succumbed to infection, precluding further sampling. In contrast, both the mRNA-H and LAV groups exhibited markedly lower RNA levels across all swab types throughout the observation period.

At necropsy, viral RNA was quantified in major organs (Fig. 7D). PBS animals harbored high viral loads in the brain, lung, spleen, liver, kidney, and bladder, indicating systemic dissemination. The mRNA-H group showed significantly reduced viral RNA across all tested organs, whereas reductions in the LAV group were less pronounced. Viral RNA was also examined in intestinal tissues, including the duodenum, jejunum, ileum, cecum, colon, rectum, and mesenteric lymph nodes (Fig. 7E). The PBS group exhibited the highest viral burdens, particularly in the rectum and mesenteric lymph nodes. In contrast, the mRNA-H group displayed a dramatic reduction in RNA levels, with rectal tissue and mesenteric lymph nodes showing highly significant decreases compared with PBS controls (*P* < 0.001).

Collectively, these findings indicate that the CDV-H mRNA-LNP vaccine not only prevented overt disease but also suppressed viral shedding and substantially limited systemic and mucosal viral dissemination, outperforming the live-attenuated vaccine.

**Discussion**

In this study, we demonstrated that the CDV-H mRNA-LNP vaccine was well tolerated and highly immunogenic in raccoon dogs, inducing potent

virus-specific antibody and CD4<sup>+</sup> T-cell responses and conferring complete protection against a lethal CDV challenge. Vaccinated animals developed robust H protein-binding and neutralizing antibodies within 3–4 weeks post-vaccination, whereas controls remained seronegative. Following exposure to virulent CDV, all immunized raccoon dogs survived without fever or clinical signs and exhibited minimal pathology, while unvaccinated controls experienced severe distemper with 100% mortality. Notably, the mRNA vaccine provided superior protection as evidenced by reduced clinical manifestations, better preservation of appetite and more rapid viral clearance. Collectively, these findings demonstrate that a two-dose regimen CDV-H mRNA-LNP formulation can safely elicit strong humoral immunity and provide complete protection from clinical disease in raccoon dogs.

Raccoon dogs were selected as the target species because of their critical role in CDV epidemiology and pathogenesis. As widely farmed fur animals in Asia and Europe, they act as important reservoir for CDV<sup>40</sup>. Experimental studies have shown that raccoon dogs develop extremely severe disease, with reported 100% mortality within 15 days post-infection—far exceeding the mortality rates in foxes (40%) or mink (0%)<sup>7</sup>. Field surveys also indicate that CDV prevalence is significantly higher in raccoon dogs than in other carnivores<sup>9,41</sup>. By contrast, domestic dogs, such as beagles, are routinely vaccinated and therefore generally more resistant, making them less suitable as stringent models for vaccine evaluation. Thus, raccoon dogs provide both a biologically relevant and economically important host species in which to assess CDV vaccine efficacy<sup>7</sup>. Commercial CDV vaccines developed for mink have historically been adapted “off-label” in raccoon dogs, where they elicit antibody responses with acceptable safety<sup>42</sup>. However, such vaccines were not optimized for this host and may provide suboptimal protection. Our study advances this field by applying an mRNA platform specifically tailored for raccoon dogs, offering both a novel strategy for disease control in fur farming and a potential tool for wildlife conservation.

The observation of 100% protection in our vaccinated group is consistent with classical live-attenuated CDV vaccines, which are known to confer sterile immunity in susceptible hosts. For instance, the commercial attenuated Onderstepoort CDV vaccine provided complete protection

ferrets, with all vaccinated animals surviving without clinical signs, whereas all unvaccinated controls succumbed to infection<sup>43</sup>. Importantly, our mRNA vaccine achieved a comparable survival outcome in raccoon dogs while circumventing the inherent safety concerns of live-attenuated vaccines, such as the potential for residual virulence. In contrast, alternative strategies have not consistently achieved such complete efficacy. For example, a DNA vaccine encoding CDV H in combination with an IFN- $\gamma$  adjuvant elicited neutralizing antibodies in ferrets but result in only 75% survival after challenge, with surviving animals still exhibiting viral shedding and pathological changes<sup>20</sup>. By comparison, our mRNA vaccine induced higher antibody titers, provided complete protection, and prevented both disease and viral dissemination. Similarly, while inactivated and live-attenuated vaccines can protect CDV-naïve animals, they often require multiple doses or prime-boost regimens to achieve immune responses comparable to those elicited by our two-dose mRNA vaccine.

Our findings also support the central role of humoral immunity in CDV protection. Previous vaccination trials in fur animals demonstrated that commercial CDV vaccines induce strong neutralizing antibody response in raccoon dogs and related species<sup>42</sup>. Consistent with these observations, our mRNA vaccine elicited high H-specific and neutralizing antibody titers within 3–4 weeks, whereas controls failed to mount comparable responses. Moreover, we detected an increase in CD4<sup>+</sup> T-cell proportions following immunization, suggesting that the vaccine also stimulated helper T-cell activity. This aligns with the established paradigm that CDV H protein-based vaccines predominantly induce antibody-mediated (Th2-biased) immunity, while cellular responses contribute to optimal protection.

When compared with prior studies in farmed carnivores, the advantages of the mRNA vaccine became particularly evident. Standard mink distemper vaccines have been used safely in raccoon dogs and are capable of eliciting antibody responses, but our challenge experiments demonstrated that the mRNA-LNP vaccine conferred at least equivalent survival benefits and superior mucosal and gastrointestinal protection<sup>42</sup>. Notably, the absence of diarrhea, maintenance of appetite, and preservation of gut histology in mRNA-vaccinated animals indicate a higher level of protective efficacy than that typically observed with inactivated or live-attenuated vaccines. Collectively, these findings suggest that mRNA-based delivery of the H antigen can elicit a more robust and comprehensive immune response compared with some conventional vaccine formulations.

Despite these promising results, several limitations should be noted. First, the study involved relatively small group sizes, and only a single homologous viral strain was used for challenge. Second, animals were young and healthy, so vaccine efficacy in older or immunocompromised individuals, or in the presence of maternal antibodies, remains untested. Third, immune responses were evaluated only up to six weeks post-boost, leaving the durability of protection beyond this period unknown. Fourth, our immunological assessment focused primarily on serology and basic CD4/CD8 phenotyping; we did not evaluate mucosal immunity (e.g. secretory IgA) or memory responses, or epitope-specific T-cell subsets.

Furthermore, the cross-lineage breadth of the antibody response requires further investigation to determine whether the vaccine could provide protection against diverse CDV genotypes<sup>33,44</sup>.

To further characterize this aspect, the H protein mRNA sequence used in this study was derived from the CDV-HBF-1 strain, which belongs to the Asia-1 genotype—the dominant lineage currently circulating in China. Its H gene shares 91.5–99.8% nucleotide identity with other Asia-1 field isolates and approximately 90.1–91.4% identity with commercial live vaccines used in fur animals (America-1 strains), indicating limited antigenic variation within the Asia-1 lineage<sup>45–47</sup>. To assess cross-reactivity, we conducted additional neutralization assays using the CDV3-CL strain, which yielded results consistent with those obtained for CDV-HBF-1, suggesting comparable neutralizing antibody responses across strains within the Asia-1 genotype. Based on current epidemiological evidence and the conserved nature of the H protein, our findings support that the mRNA vaccine provides cross-protection among circulating Asia-1 variants.

From an immunological perspective, detailed analyses—including cytokine profiling, ELISPOT, pseudotype neutralization with different receptors, or B-cell ELISPOT—could help identify correlates of protection. If any reactogenicity signals are detected, formulation adjustments, such as modifying lipid ratios or including adjuvants, may enhance safety. These investigations would inform optimization of dosing schedules and vaccine deployment<sup>48,49</sup>. Additionally, evaluating antibody cross-reactivity across different CDV strains is essential. Previous studies have reported cross-neutralization between vaccine and field strains<sup>50</sup>. Determining whether neutralizing antibodies elicited by the mRNA-LNP vaccine effectively recognize diverse strains will ensure its potential to confer broad protection, thereby increasing its utility as a tool for controlling CDV outbreaks in wildlife populations.

This study opens several avenues for further investigation. A primary objective is to evaluate long-term protection: whether vaccinated raccoon dogs maintain immunity against CDV after six months or one year, and whether booster doses are required. It would also be valuable to assess the mRNA vaccine in other CDV-susceptible species, such as ferrets, foxes, and minks, to determine its cross-species applicability. The potential for combination vaccines, incorporating CDV mRNA with other antigens relevant to fur-farm pathogens, warrants exploration. Given the flexibility of mRNA platforms, constructs encoding variant H genes from diverse lineages—or antigen cocktails including H plus F or N proteins—could be evaluated to broaden immune coverage. Mechanistic studies might clarify which LNP components drive the observed Th2-biased and whether inclusion of specific immunostimulants could enhance cellular immunity<sup>51</sup>. From a practical level, considerations of vaccine manufacturing, stability, and cold-chain logistics are essential for deployment in raccoon dog populations. Additionally, ecological and epidemiological studies could evaluate the broader impact of vaccination on CDV transmission, particularly its potential to reduce spillover into wildlife and zoo populations, as documented in prior distemper outbreaks<sup>41</sup>.

In summary, the CDV-H mRNA-LNP vaccine elicited robust, protective immunity in raccoon dogs. This work extends previous CDV vaccine research by demonstrating the efficacy of an mRNA platform in a highly susceptible carnivore species, supporting its potential as a promising candidate for future development and evaluation in fur-animal farms and wildlife conservation efforts.

## Methods

### Design and preparation of CDV-H mRNA-LNP vaccine

The extracellular domain (ECD) of the H protein from CDV was selected as the immunogen in this study. To enhance secretion efficiency and structural stability, a SP and the T $\beta$ tetra were fused at the N-terminus of the antigen. The antigen coding sequence was cloned into a DNA plasmid containing 5' and 3' untranslated regions (UTRs) and a poly(A) tail to improve mRNA stability and translation efficiency.

The mRNA was synthesized by *in vitro* transcription (IVT) using T7 RNA polymerase, with a Cap 1 analogue co-transcriptionally added to enhance translational efficiency. Transcription products were purified by lithium chloride precipitation or column chromatography and resuspended in buffer for LNP formulation. LNPs were prepared using a defined lipid composition consisting of SM102, DSPC, cholesterol, and DMG-PEG2000 at a molar ratio of 50:10:38.5:1.5. The mRNA was dissolved in 10 mM sodium citrate buffer (pH 4.0) and rapidly mixed with the ethanol-dissolved lipid phase at a 1:3 volume ratio using a microfluidic mixing system to form nanoparticles. The resulting LNP formulation was exchanged into phosphate-buffered saline (PBS, pH 7.4), concentrated and stored under the appropriate conditions until required.

### *In vivo* delivery and expression validation of the mRNA vaccine

Five micrograms of fluorescently labeled CDV H protein mRNA-LNP vaccine was administered via intramuscular injection into 6-week-old BALB/c mice (Beijing Vital River Laboratory Animal Technology Co., Ltd.), with PBS-injected mice serving as negative controls. Six hours post-

injection, mice were anesthetized with isoflurane gas and intraperitoneally injected with 3 mg D-luciferin (dissolved in PBS). In vivo bioluminescence imaging was performed using an IVIS imaging system (PerkinElmer, USA) 10 minutes after luciferin administration to capture and quantify fluorescence signals, evaluating the biodistribution of the mRNA-LNP at the injection site and other tissues.

The particle size and distribution uniformity of the LNP were measured by dynamic light scattering (DLS) using a BeNano 90 Zeta instrument (Bettersize Instruments Ltd., Dandong, China). Samples were diluted in PBS buffer (pH 7.4) and measured at 25 °C. The average hydrodynamic diameter and polydispersity index (PDI) were recorded, and the autocorrelation function ( $g^2-1$ ) curve and intercept value were analyzed to assess sample uniformity and signal-to-noise ratio. All measurements were performed in triplicate, and average values were reported.

For in vitro expression validation, CHO cells cultured in suspension were adjusted to a density of  $4 \times 10^6$  cells/mL. When the desired density was reached, cells were transfected with CDV-H mRNA-LNP at a final concentration of 6 µg/mL. Cells were further cultured for 24 hours post-transfection, with untreated cells serving as negative controls. Expression of the CDV H protein was detected by indirect immunofluorescence (IF) staining using a rabbit polyclonal antibody as the primary antibody, FITC-conjugated goat anti-rabbit IgG as the secondary antibody, and DAPI for nuclear staining. Western blot (WB) analysis was conducted on cell lysates to confirm the molecular weight and glycosylation status of the expressed H protein.

### Mouse immunization and sampling

Female BALB/c mice aged 6 to 8 weeks, weighing approximately 18–22 g, were intramuscularly immunized with 50 µg of formulated CDV H protein mRNA-LNP vaccine on Days 0 and 21<sup>30</sup>. The control group received PBS injections. Five mice were randomly selected and assigned to each group. Blood samples were collected via tail vein on Days 0, 21, 28, and 42 post-immunization<sup>52</sup>. At 42 days post-immunization (dpi), mice were euthanized, and spleens were aseptically harvested for subsequent analyses.

All animal experiments were conducted in accordance with the guidelines and regulations of the Experimental Animal Ethics Committee of the Institute of Special Animal and Plant Sciences, Chinese Academy of Agricultural Sciences (approval number ISAPSAEC-2024-031RCDV). All procedures were approved by the committee, and every effort was made to minimize animal suffering and to reduce the number of animals used.

### Serological assays

Serum samples were separated by centrifugation and stored at –20 °C until use. CDV H protein-specific antibodies in mouse sera were measured by indirect enzyme-linked immunosorbent assay (ELISA). Briefly, purified CDV H protein was coated onto 96-well plates overnight at 4 °C. After blocking, diluted serum samples were added and incubated, followed by horseradish peroxidase (HRP)-conjugated secondary antibody. Color development was performed using TMB substrate, and absorbance was measured at 450 nm. For indirect immunofluorescence assay, Vero cells were cultured on coverslips, fixed with paraformaldehyde, and incubated with diluted mouse sera. After washing, FITC-conjugated goat anti-mouse IgG secondary antibody (BioLegend) was applied. Cell nuclei were counterstained with DAPI. Fluorescent images were captured using a fluorescence microscope.

### Flow cytometry analysis of splenic lymphocytes

Single-cell suspensions of splenic lymphocytes were prepared using a spleen lymphocyte isolation kit (Beijing Solarbio Science & Technology Co., Ltd.) according to the manufacturer's instructions. Cells were counted and adjusted to an appropriate concentration. Approximately  $1 \times 10^5$  cells were incubated with fluorochrome-conjugated antibodies against CD3, CD4, and CD8 (all from BioLegend) at 4 °C in the dark for 30 minutes. After washing, samples were analyzed using a BD flow cytometer. Data were processed with FlowJo software, gating on CD3<sup>+</sup> lymphocytes to further analyze CD4<sup>+</sup> and

CD8<sup>+</sup> T cell subsets. Statistical significance was assessed by appropriate methods.

### Immunization protocol and sample collection in raccoon dogs

Raccoon dogs aged 6–8 weeks were randomly divided into three groups: the PBS group, the mRNA-H group, and the LAV group, with 5 raccoon dogs in each group<sup>52,53</sup>. The mRNA-H group received intramuscular injections of the mRNA-H vaccine at Days 0 and 21, with a dose of  $10^{3.5}$  µg per administration. The LAV group was immunized with the live-attenuated vaccine following the same schedule. Control animals in the PBS group received equivalent volumes of PBS. Blood samples were collected at scheduled time points (Days 0, 21, 28, and 42 post-immunization). At 42 dpi, animals were challenged with CDV (designated as Day 0 post-challenge) and euthanized after 14 days of monitoring (Day 56 post-immunization) for tissue collection. During the immunization period, local reactivity, behavioral status, feed intake, and fecal consistency were monitored in real time, and body temperature was measured at each sampling point.

### Monitoring of safety and reactivity

Following each immunization, local injection site reactions (e.g., erythema, swelling), behavioral status (e.g., lethargy, activity level), feed intake, and body temperature were recorded daily for 7 consecutive days. Fecal consistency was monitored for 14 days post-immunization. All parameters were assessed using predefined scoring criteria to systematically evaluate the local and systemic reactivity and overall safety of the vaccine.

### Serological evaluation of raccoon dogs post immunization

At 42 days post-immunization, serum samples were collected from raccoon dogs via venous blood draw for antibody analysis. CDV H protein-specific antibodies were detected using indirect ELISA. Plates were coated with recombinant H protein, and serum samples (diluted 1:100) were incubated, followed by addition of an HRP-conjugated goat anti-dog IgG secondary antibody (purchased from Beijing Bioss Biotechnology Co., Ltd). After substrate reaction, absorbance was measured at 450 nm.

To assess the levels of neutralizing antibodies, we conducted a virus neutralization assay using a CDV-HBF-1 strain preserved in our laboratory. First, the serum was serially diluted and incubated with 200 50% Tissue Culture Infectious Doses (TCID<sub>50</sub>) of CDV. Subsequently, the mixture was added to Vero cells, which are sensitive to CDV. The cells were cultured at 37 °C for 5 days. If the antibodies in the serum did not neutralize the virus, the virus would infect the Vero cells and cause cytopathic effects (CPE). We observed the cells under a microscope, recorded whether CPE occurred in each well, and calculated the neutralizing antibody titers using the Reed-Muench method. These titers reflect the strength of the neutralizing ability of the serum antibodies and provide crucial data for evaluating the effectiveness of the vaccine-induced immune response against CDV.

### Analysis of peripheral blood lymphocyte subsets

At 42 days dpi, peripheral blood samples were collected from raccoon dogs via venipuncture. Peripheral blood mononuclear cells (PBMCs) were isolated using a commercial isolation kit for small carnivores (Solarbio, Beijing, China). Cells were resuspended and stained with fluorochrome-conjugated antibodies: anti-CD3-FITC and anti-CD4-PE (BioLegend, USA). We performed flow cytometric analysis using a BD flow cytometer, gating on CD3<sup>+</sup> lymphocytes to determine the proportion of CD4<sup>+</sup> T cell subpopulations. All samples were analyzed in triplicate with unstained controls to ensure data reliability. All samples included unstained controls and were analyzed in triplicate to ensure data reliability. CD8<sup>+</sup> T cell analysis was not performed due to the lack of validated antibodies for raccoon dog species.

### Virus challenge and survival monitoring

After the completion of the immunization regimen, raccoon dogs were challenged with CDV. The CDV-HBF-1 strain, which was maintained and propagated in our laboratory, had a viral titer of  $10^{5.5}$  TCID<sub>50</sub>/mL. Each

**Table 1 | Primer sequences**

	Tm	GC%	Length(bp)	Sequences
Primer-F	61.3	66	18	5'-cgggaccaacccccactt-3'
Primer-R	55.5	45	24	5'-caccogggattaggactataatga-3'

animal received an intramuscular injection of 1 mL of virus suspension containing 100 ID<sub>50</sub> per animal into the thigh muscle. The day of the challenge was designated as Day 0 (corresponding to Day 42 post-immunization). The animals were monitored daily for 14 consecutive days post-challenge (up to Day 56 post-immunization), and their daily survival status was recorded. All observations were conducted by personnel blinded to the treatment groups to prevent bias. The survival data were used to generate Kaplan–Meier survival curves.

### Post-challenge clinical monitoring and sample collection

Following viral challenge at 42 dpi (designated as Day 0 post-challenge), raccoon dogs were observed daily for 14 consecutive days (up to Day 56 post-immunization) to assess clinical signs and disease severity. Body temperature was measured once per day at the axillary site, and a scoring system was used to evaluate the severity of clinical parameters including feed intake, behavioral status, fecal consistency, eyelid and conjunctival changes, and nasal discharge. Additionally, ocular swabs, nasal swabs, and anal swabs were collected every 48 h (on Days 2, 4, 6, 8, 10, 12, and 14 post-challenge) using separate sterile swabs for each site. Swabs were immediately placed into viral transport medium and stored at  $-80^{\circ}\text{C}$  for subsequent antigen or viral nucleic acid testing.

### CDV antigen detection in anal swabs

Anal swabs were collected from surviving raccoon dogs at 14 days post-challenge (dpc), and from deceased animals immediately upon death. Sterile swabs were gently rotated around the perianal area, then placed into viral transport medium and transported to the laboratory at room temperature. A CDV antigen rapid test cassette (Shanghai Kuailing Biotechnology Co., Ltd.) was used according to the manufacturer's instructions. Swabs were mixed thoroughly in the provided buffer, and an appropriate volume (per kit instructions) of sample eluate was applied to the sample well of the test cassette. Test results were read at 5–10 minutes post-application. Interpretation criteria were as follows: appearance of only the control line (C) indicated a negative result; absence of the control line rendered the test invalid; concurrent appearance of both test (T) and control (C) lines indicated a positive result, with the intensity of the T line reflecting relative antigen load. Any faint T line appearing after 30 minutes was considered negative. Each animal's result was recorded accordingly.

### Tissue collection and gross pathology

At 14 dpc or immediately upon death, raccoon dogs were euthanized and subjected to a full necropsy. Major organs—including brain, lungs, and spleen—as well as the entire intestinal tract (duodenum, jejunum, ileum, cecum, colon, rectum) and mesenteric lymph nodes were carefully excised. Each organ was inspected grossly for evidence of hemorrhage, edema, ulceration, necrosis, enlargement, or other visible lesions. Representative lesions were photographed under standardized lighting with a scale for documentation.

### Tissue fixation, processing, and H&E staining

Excised tissues were immediately placed in 10% neutral buffered formalin and fixed for at least 48 hours. Following fixation, tissues were dehydrated through graded alcohols, cleared in xylene, and embedded in paraffin. Sections of 4–5  $\mu\text{m}$  thickness were cut and mounted on glass slides. After deparaffinization and rehydration, sections were stained with hematoxylin and eosin (H&E) using standard procedures. Sections from brain, lung, spleen, and all intestinal segments (duodenum, jejunum, ileum, cecum, colon, rectum) were examined microscopically, and representative fields illustrating characteristic lesions were photographed.

### Semi-quantitative pathological scoring

All tissue lesions were evaluated by assigning scores to reflect the severity of pathological changes. Two experienced veterinary pathologists, blinded to the treatment groups, independently scored each slide; discrepancies were reconciled by joint review to reach a consensus. Mean scores  $\pm$  SEM were calculated for each group ( $n = 5$  per group).

### Quantification of CDV viral load by qPCR

Tissue samples were frozen in liquid nitrogen, then homogenized with 1 mL sterile PBS and steel beads using a tissue grinder for six 30 s cycles. The homogenate was centrifuged at 12,000 rpm for 5 minutes at  $4^{\circ}\text{C}$ . RNA was extracted from 400  $\mu\text{L}$  supernatant using a commercial viral RNA extraction kit (Xi'an Tianlong Technology) and automatic extractor, following the manufacturer's instructions. One-step RT-qPCR was performed using the TB Green kit (Dalian Bao Biological Engineering) with CDV-specific primers (Table 1). Quantification was based on a standard curve from serial dilutions of known templates.

### Clinical monitoring, humane endpoints, and euthanasia procedure

At 42 dpi, raccoon dogs were challenged with 100 ID<sub>50</sub> of CDV HBF-1. Post-challenge clinical signs were evaluated twice daily for 14 days by two blinded observers using a predefined 10-point composite scoring system assessing respiratory distress (0:  $<40$  breaths/min; 1: 40–50; 2: 51–60; 3:  $>60$  with abdominal effort), neurological signs (0: normal; 1: mild ataxia or intermittent tremor; 2: persistent tremor, disorientation, or head tilt; 3: paralysis or seizures), systemic status (0: normal activity and appetite; 1: appetite decreased  $\leq 30\%$ ; 2: depression or anorexia  $>24$  h; 3: recumbency or severe dehydration  $>10\%$ ), and fever/hypothermia (0: 38.0–39.5  $^{\circ}\text{C}$ ; 1:  $>39.5^{\circ}\text{C}$  or  $<38.0^{\circ}\text{C}$ , or abnormal temperature lasting  $>24$  h). Animals meeting humane endpoint criteria were assigned a fixed clinical score of 10 for that day.

Death was not used as an experimental endpoint. Animals were humanely euthanized immediately if they met any humane endpoint, including severe dyspnea (respiratory score = 3), seizures or paralysis (neurological score = 3), recumbency or inability to rise for  $>12$  h, anorexia for  $>48$  h, sustained fever  $\geq 40^{\circ}\text{C}$  for  $>48$  h or hypothermia  $<38.0^{\circ}\text{C}$ , 15–20% body-weight loss, severe diarrhea with dehydration, or a composite clinical score  $\geq 8$  at any single assessment.

At the study endpoint or upon reaching humane endpoints, euthanasia was performed using sodium pentobarbital prepared as a 3% solution. For mice, euthanasia was performed via intraperitoneal injection at 80 mg/kg; for raccoon dogs, via intravenous injection into the saphenous vein at 200 mg/kg. Death was confirmed by the absence of respiration and heart-beat for  $\geq 5$  minutes and the loss of corneal and pedal reflexes, followed by cervical dislocation as a secondary method to ensure complete euthanasia.

### Statistical analysis

All statistical analyses were performed using GraphPad Prism 8.0 software. Prior to formal testing, the Shapiro–Wilk test was used to assess data normality, and Levene's test was used to evaluate homogeneity of variance, ensuring compliance with the assumptions of parametric analyses. For pairwise comparisons between two groups, two-tailed Student's *t*-tests were applied, consistent with the primary objective of assessing vaccine-induced improvements relative to control animals. For repeated-measures variables (e.g., temporal changes in body temperature, viral load, and clinical scores) and semi-quantitative data (e.g., pathological scoring), two-way repeated-measures ANOVA followed by Tukey's post-hoc test was used to assess group effects, time effects, and their interactions. All results are presented as mean  $\pm$  standard error of the mean (SEM). Statistical significance was defined as:  $P < 0.05$ ;  $*P < 0.01$ ;  $**P < 0.001$ ; ns, not significant.

### Rationale for group number and sample size determination

This study was conducted using three experimental groups (PBS control, mRNA-H vaccine, and LAV), determined by the scientific needs of the

study design<sup>1</sup>: The PBS group served as a negative control to characterize the natural course of CDV infection (e.g., clinical signs, disease progression, and viral replication) in unvaccinated animals<sup>2</sup>. The mRNA-H group was the test group evaluating the immunogenicity, safety, and protective efficacy of the CDV-H mRNA-LNP vaccine<sup>3</sup>. The LAV group served as a positive control using a licensed CDV vaccine to benchmark the mRNA platform against an established vaccine modality.

The sample size ( $n = 5$  animals per group for both raccoon dogs and mice) was determined based on three considerations<sup>1</sup>: Adherence to the 3 R principle (Reduction), minimizing animal use while ensuring statistical reliability<sup>2</sup>. Reference to the sample-size logic used by Xu et al. (2025) in raccoon dog viral challenge studies<sup>53</sup>, which provided species-relevant guidance<sup>3</sup>. Reference to the vaccine efficacy sample-size framework proposed by Zhao et al. (2024)<sup>30</sup>, in which the statistical principles for ensuring adequate power in mRNA vaccine studies are applicable to both mice and raccoon dogs.

The final study design (three groups,  $n = 5$  per group) ensures scientific robustness while complying with ethical approval from the Experimental Animal Ethics Committee of the Institute of Special Animal and Plant Sciences, Chinese Academy of Agricultural Sciences.

## Data availability

The data that support the findings of this study are available upon request from the corresponding author.

Received: 21 June 2025; Accepted: 2 December 2025;

Published online: 14 December 2025

## References

- Duque-Valencia, J., Sarute, N., Olarte-Castillo, X. A. & Ruiz-Sáenz, J. Evolution and interspecies transmission of canine distemper virus—an outlook of the diverse evolutionary landscapes of a multi-host virus. *Viruses* **11**, 582 (2019).
- Carbone, F. et al. Divergent immunomodulatory effects of recombinant and urinary-derived FSH, LH, and hCG on human CD4+ T cells. *J. Reprod. Immunol.* **85**, 172–179 (2010).
- Welter, J., Taylor, J., Tartaglia, J., Paoletti, E. & Stephensen, C. B. Mucosal vaccination with recombinant poxvirus vaccines protects ferrets against symptomatic CDV infection. *Vaccine* **17**, 308–318 (1999).
- Wilkes, R. P. Canine distemper virus in endangered species: species jump, clinical variations, and vaccination. *Pathogens* **12**, 57 (2022).
- Loots, A. K., Mitchell, E., Dalton, D. L., Kotzé, A. & Venter, E. H. Advances in canine distemper virus pathogenesis research: a wildlife perspective. *J. Gen. Virol.* **98**, 311–321 (2017).
- Prpić, J., Lojkić, I., Keros, T., Krešić, N. & Jemeršić, L. Canine distemper virus infection in the free-living wild canines, the red fox (*vulpes vulpes*) and jackal (*canis aureus moreoticus*), in Croatia. *Pathogens* **12**, 833 (2023).
- Zhao, J. et al. Pathogenesis of canine distemper virus in experimentally infected raccoon dogs, foxes, and minks. *Antivir. Res.* **122**, 1–11 (2015).
- Kennedy, J. M. et al. Canine and phocine distemper viruses: global spread and genetic basis of jumping species barriers. *Viruses* **11**, 944 (2019).
- Liang, J. et al. Prevalence of canine distemper in minks, foxes and raccoon dogs from 1983 to 2023 in Asia, North America, South America and Europe. *Front. Vet. Sci.* **11**, 1394631 (2024).
- Martella, V. et al. Heterogeneity within the hemagglutinin genes of canine distemper virus (CDV) strains detected in Italy. *Vet. Microbiol.* **116**, 301–309 (2006).
- Woma, T. Y., van Vuuren, M., Bosman, A.-M., Quan, M. & Oosthuizen, M. Phylogenetic analysis of the haemagglutinin gene of current wild-type canine distemper viruses from South Africa: lineage Africa. *Vet. Microbiol.* **143**, 126–132 (2010).
- Panzer, Y., Sarute, N., Iraola, G., Hernández, M. & Pérez, R. Molecular phylogeography of canine distemper virus: geographic origin and global spreading. *Mol. Phylogenet. Evol.* **92**, 147–154 (2015).
- Nikolin, V. M., Wibbelt, G., Michler, F.-U. F., Wolf, P. & East, M. L. Susceptibility of carnivore hosts to strains of canine distemper virus from distinct genetic lineages. *Vet. Microbiol.* **156**, 45–53 (2012).
- Zhao, J. et al. Emergence of canine distemper virus strains with two amino acid substitutions in the haemagglutinin protein, detected from vaccinated carnivores in North-Eastern China in 2012–2013. *Vet. J.* **200**, 191–194 (2014).
- Zhao, J.-J. et al. Phylogenetic analysis of the haemagglutinin gene of canine distemper virus strains detected from breeding foxes, raccoon dogs and minks in China. *Vet. Microbiol.* **140**, 34–42 (2010).
- Wyss, M. et al. Efficient recovery of attenuated canine distemper virus from cDNA. *Virus Res.* **316**, 198796 (2022).
- Bronson, E., Deem, S. L., Sanchez, C. & Murray, S. Serologic response to a canarypox-vectored canine distemper virus vaccine in the giant panda (*Ailuropoda melanoleuca*). *J. Zoo. Wildl. Med.* **38**, 363–366 (2007).
- Wright, M. L., Livieri, T. M. & Santymire, R. M. Recombitek canine distemper vaccine as an alternative for Purevax distemper vaccine in endangered black-footed ferrets (*Mustela nigripes*). *J. Zoo. Wildl. Med.* **53**, 194–199 (2022).
- Rendon-Marin, S. & Ruiz-Saenz, J. Universal peptide-based potential vaccine design against canine distemper virus (CDV) using a vaccinomic approach. *Sci. Rep.* **14**, 16605 (2024).
- Zhao, J. et al. DNA vaccine co-expressing hemagglutinin and IFN- $\gamma$  provides partial protection to ferrets against lethal challenge with canine distemper virus. *Viruses* **15**, 1873 (2023).
- Wang, J. et al. Immunogenicity and protective efficacy of a novel bacterium-like particle-based vaccine displaying canine distemper virus antigens in mice and dogs. *Microbiol. Spectr.* **12**, e0347723 (2024).
- Liu, L. et al. A bacterium-like particle vaccine displaying envelope proteins of canine distemper virus can induce immune responses in mice and dogs. *Viruses* **16**, 549 (2024).
- Shoushtari, M. et al. Heterologous Prime-Boost immunization with Adenoviral vector and recombinant subunit vaccines strategies against dengue virus type2. *Int. Immunopharmacol.* **148**, 114032 (2025).
- Le, T., Sun, C., Chang, J., Zhang, G. & Yin, X. mRNA vaccine development for emerging animal and zoonotic diseases. *Viruses* **14**, 401 (2022).
- Liu, D. et al. Study on immunogenicity of recombinant ferritin hemagglutinin of canine distemper virus. *Viro. J.* **22**, 260 (2025).
- Pardi, N., Hogan, M. J., Porter, F. W. & Weissman, D. mRNA vaccines—a new era in vaccinology. *Nat. Rev. Drug Discov.* **17**, 261–279 (2018).
- Gouma, S. et al. Nucleoside-modified mRNA-based influenza vaccines circumvent problems associated with H3N2 vaccine strain egg adaptation. *J. Virol.* **97**, e0172322 (2023).
- Medina-Magües, L. G. et al. mRNA vaccine protects against Zika virus. *Vaccines* **9**, 1464 (2021).
- Fazel, F. et al. The mRNA vaccine platform for veterinary species. *Vet. Immunol. Immunopathol.* **274**, 110803 (2024).
- Zhao, Y. et al. PEDV-spike-protein-expressing mRNA vaccine protects piglets against PEDV challenge. *mBio* **15**, e0295823 (2024).
- Zhou, L. et al. The mRNA vaccine expressing single and fused structural proteins of porcine reproductive and respiratory syndrome induces strong cellular and humoral immune responses in BalB/C mice. *Viruses* **16**, 544 (2024).
- Zhao, J. & Ren, Y. Multiple receptors involved in invasion and neuropathogenicity of canine distemper virus: a review. *Viruses* **14**, 1520 (2022).

33. Wang, W. et al. Development of a monoclonal antibody recognizing novel linear neutralizing epitope on H protein of canine distemper virus vaccine strains (America-1 genotype). *Int. J. Biol. Macromol.* **246**, 125584 (2023).
34. von Messling, V. & Cattaneo, R. Amino-terminal precursor sequence modulates canine distemper virus fusion protein function. *J. Virol.* **76**, 4172–4180 (2002).
35. Kalbermatter, D. et al. Cryo-EM structure of the prefusion state of canine distemper virus fusion protein ectodomain. *J. Struct. Biol. X* **4**, 100021 (2020).
36. Z B, Y W, Q P, X X, L X. Development of CDV-specific monoclonal antibodies for differentiation of variable epitopes of nucleocapsid protein. *Veterinary Microbiol.* **211** (2017).
37. Chen, F. et al. Canine distemper virus N protein induces autophagy to facilitate viral replication. *BMC Vet. Res.* **19**, 60 (2023).
38. Suzuki, Y. et al. Splenic B cell-targeting lipid nanoparticles for safe and effective mRNA vaccine delivery. *J. Control Release* **382**, 113687 (2025).
39. Tai, W. et al. An mRNA-based T-cell-inducing antigen strengthens COVID-19 vaccine against SARS-CoV-2 variants. *Nat. Commun.* **14**, 2962 (2023).
40. Lanszki, Z. et al. Prolonged infection of canine distemper virus in a mixed-breed dog. *Vet. Sci.* **8**, 61 (2021).
41. Feng, N. et al. Fatal canine distemper virus infection of giant pandas in China. *Sci. Rep.* **6**, 27518 (2016).
42. Rikula, U., Pänkälä, L., Jalkanen, L. & Sihvonen, L. Distemper vaccination of farmed fur animals in Finland. *Prev. Vet. Med.* **49**, 125–133 (2001).
43. Wimsatt, J., Jay, M. T., Innes, K. E., Jessen, M. & Collins, J. K. Serologic evaluation, efficacy, and safety of a commercial modified-live canine distemper vaccine in domestic ferrets. *Am. J. Vet. Res.* **62**, 736–740 (2001).
44. Dos Santos, C. P. et al. Epitope mapping and a candidate vaccine design from canine distemper virus. *Open Vet. J.* **14**, 1019–1028 (2024).
45. Feng, C. et al. Persistent and severe viral replication in PBMCs with moderate immunosuppression served an alternative novel pathogenic mechanism for canine morbillivirus. *Microbiol. Spectr.* **11**, e0406022 (2023).
46. Guo, L. et al. Phylogenetic analysis of the haemagglutinin gene of canine distemper virus strains detected from giant panda and raccoon dogs in China. *Virol. J.* **10**, 109 (2013).
47. Anis, E., Newell, T. K., Dyer, N. & Wilkes, R. P. Phylogenetic analysis of the wild-type strains of canine distemper virus circulating in the United States. *Virol. J.* **15**, 118 (2018).
48. Wang, J. et al. Trivalent mRNA vaccine against SARS-CoV-2 and variants with effective immunization. *Mol. Pharm.* **20**, 4971–4983 (2023).
49. Ma, Q. et al. SARS-CoV-2 bivalent mRNA vaccine with broad protection against variants of concern. *Front. Immunol.* **14**, 1195299 (2023).
50. Mochizuki, M., Motoyoshi, M., Maeda, K. & Kai, K. Complement-mediated neutralization of canine distemper virus in vitro: cross-reaction between vaccine Onderstepoort and field KDK-1 strains with different hemagglutinin gene characteristics. *Clin. Diagn. Lab Immunol.* **9**, 921–924 (2002).
51. Ronk, A. J. et al. A Lassa virus mRNA vaccine confers protection but does not require neutralizing antibody in a guinea pig model of infection. *Nat. Commun.* **14**, 5603 (2023).
52. Kackos, C. M. et al. mRNA Vaccine Mitigates SARS-CoV-2 Infections and COVID-19. *Microbiol. Spectr.* **11**, e0424022 (2023).
53. Xu L. et al. Residues 27T and 297A in VP2 contribute to the enhanced replication and pathogenicity of raccoon dog parvovirus. *J. Virol.* **e0101225** (2025).

## Acknowledgements

This work was supported by the National Key Research and Development Program of China (Grant No. 2023YFD1800700) and the Science and Technology Development Plan of Jilin Province (Grant No. 20250601046RC).

## Author contributions

All the authors contributed to the research concept and design. C.Z.: writing—original draft. C.Z. and T.H.: formal analysis, visualisation, validation, software, data curation, writing—review and editing. C.Z., T.H., D.G., S.L., W.C., X.G., Z.Z., J.L., Y.S., W.X., M.X. and J.L.: methodology, investigation. B.H., S.X. and X.B.: conceptualization, resources, data curation, supervision, funding acquisition. All authors have read and agreed to the published version of the manuscript.

## Competing interests

The authors declare no competing interests.

## Additional information

**Supplementary information** The online version contains supplementary material available at <https://doi.org/10.1038/s41541-025-01337-0>.

**Correspondence** and requests for materials should be addressed to Shi Xu, Bo Hu or Xue Bai.

**Reprints and permissions information** is available at <http://www.nature.com/reprints>

**Publisher's note** Springer Nature remains neutral with regard to jurisdictional claims in published maps and institutional affiliations.

**Open Access** This article is licensed under a Creative Commons Attribution-NonCommercial-NoDerivatives 4.0 International License, which permits any non-commercial use, sharing, distribution and reproduction in any medium or format, as long as you give appropriate credit to the original author(s) and the source, provide a link to the Creative Commons licence, and indicate if you modified the licensed material. You do not have permission under this licence to share adapted material derived from this article or parts of it. The images or other third party material in this article are included in the article's Creative Commons licence, unless indicated otherwise in a credit line to the material. If material is not included in the article's Creative Commons licence and your intended use is not permitted by statutory regulation or exceeds the permitted use, you will need to obtain permission directly from the copyright holder. To view a copy of this licence, visit <http://creativecommons.org/licenses/by-nc-nd/4.0/>.

© The Author(s) 2025